© 2018. Published by The Company of Biologists Ltd | Journal of Experimental Biology (2018) 221, jeb178400. doi:10.1242/jeb.178400

SHORT COMMUNICATION

Relative position of the atrioventricular canal determines the electrical activation of developing reptile ventricles

Martina Gregorovicova[1], David Sedmera[1] and Bjarke Jensen[2,*]

ABSTRACT

Squamate reptiles appear to lack the specialized His–Purkinje system that enables the cardiac ventricle to be activated from apex to base as in mammals and birds. Instead, activation may simply spread from where the atrioventricular canal connects to the base. *Gja5*, which encodes Cx40, which allows fast impulse propagation, was expressed throughout the ventricles of developing anole lizards. Activation was optically recorded in developing corn snake and central bearded dragon. Early embryonic ventricles were broad in shape, and activation propagated from the base to the right. Elongated ventricles of later stages were activated from base to apex. Before hatching of the snake, the ventricle developed a cranial extension on the left and activation propagated from the base to the caudal apex and the cranial extension. In squamate reptiles, the pattern of electrical activation of the cardiac ventricle is dependent on the position of the atrioventricular canal and the shape of the ventricle.

KEY WORDS: Development, Cardiac conduction system, Heart, Optical mapping

INTRODUCTION

Heart muscle cells become electrically excited by action potentials, coupled to which is the calcium release that induces contraction (Burggren et al., 1998). In hearts of mammals and birds, the His–Purkinje system allows rapid conduction of the action potential that originates in the sinus node through specialized, large heart cells arranged in defined bundles that travel from the ventricular base (cranial) to the ventricular apex (caudal) (Davies and Francis, 1946; Dobrzynski et al., 2013). Accordingly, activation of most of the ventricular mass is from the apex towards the base (Sedmera, 2011). Molecularly, the His–Purkinje system is distinguished by the presence of the low-resistance gap junction protein Cx40, and its transcript *Gja5*, which allows fast conduction (Park and Fishman, 2017). Crocodylians appear to be the only ectotherms with a His bundle-like structure, probably because they are the only ectotherms with a full ventricular septum like mammals and birds (Jensen et al., 2018). The earliest activated part of the ventricular surface, the breakthrough of the activation, is towards the apex in the region of the ventricular septum. Crocodylians do not have a Purkinje system, as key markers, *Gja5* and *Nppb*, are not confined to a small subset of ventricular muscle but are broadly expressed (Jensen et al., 2018).

[1]Institute of Anatomy, First Medical Faculty, Charles University, 12800 Prague, and Institute of Physiology, Czech Academy of Sciences, 14220 Prague, Czech Republic. [2]Department of Medical Biology, Academic Medical Center, University of Amterdam, 1105 AZ Amsterdam, The Netherlands.

*Author for correspondence (b.jensen@amc.uva.nl)

B.J., 0000-0002-7750-8035

Received 30 January 2018; Accepted 16 April 2018

Anole lizards have a typical squamate reptile heart (Jensen et al., 2014) and ventricular activation proceeds from the base, where the atria connect to the ventricular mass, to the apex (Jensen et al., 2012). No His–Purkinje system was found (Jensen et al., 2012), although this does not rule out a role for the 5–10 dorsoventrally and caudocranially oriented sheets of myocardium that are a common feature in the center of the ventricle of ectotherms (Sedmera et al., 2003). The absence of a His–Purkinje system begs the question whether, in the lizard ventricle, current may propagate at similar velocity from its point of initiation outwards in any direction. If true, the pattern of activation in lizards may be determined largely by the shape of the ventricle and where the atria connect to this shape. Here, we tested this hypothesis on developing lizards and snakes, as their ventricles develop from early left–right broad to caudocranially elongated in late stages. We found that the first activated region was always in the vicinity of the atrioventricular junction and the last point was on the far right in the early stages and at the apex in the later stages, thus always furthest away from the atrioventricular junction.

MATERIALS AND METHODS

Animals

The handling of anole lizards (*Anolis sagrei* Duméril and Bibron 1837) and harvest of tissues complied with national and institutional guidelines and were approved by the Institutional Animal Care and Use Committee of the University of Amsterdam (DAE101617). For *in situ* hybridization, we used anole lizards of which one was adult and four were isolated from eggs and staged according to Sanger et al. (2008) (stages 7, 9, 17, 19). None of the sections shown have been published before, but other sections of the stage 19 specimen and the adult have been used in previous publications (Jensen et al., 2012, 2017). For optical mapping, we used 17 specimens of the central bearded dragon (*Pogona vitticeps* Ahl 1926) from embryonated eggs ranging in incubated age from 14 to 62 days post-oviposition and staged according to Sanger et al. (2008), and four specimens of the corn snake [*Pantherophis guttatus* (Linnaeus, 1766)] from embryonated eggs ranging in incubated age from 9 to 32 days post-oviposition and staged according to Boback et al. (2012). Under Czech Animal Protection law, handling of embryos in eggs is exempt from regulation; furthermore, only samplings followed by *in vitro* measurements of isolated hearts were performed.

In situ hybridization

We performed non-radioactive *in situ* hybridization to detect the gene transcript (*Gja5*) of the low-resistance gap junction protein Cx40 as described previously (Jensen et al., 2012, 2017). The probe was based on the sequence of the following coordinates using UCSC Genome Browser on Lizard May 2010 (Broad AnoCar2.0/anoCar2) Assembly; *Gja5* (chr3:162,064,640-162,065,729). This gene transcript marks the ventricular conduction system, or His–

Journal of Experimental Biology (2018) 221, jeb178400. doi:10.1242/jeb.178400

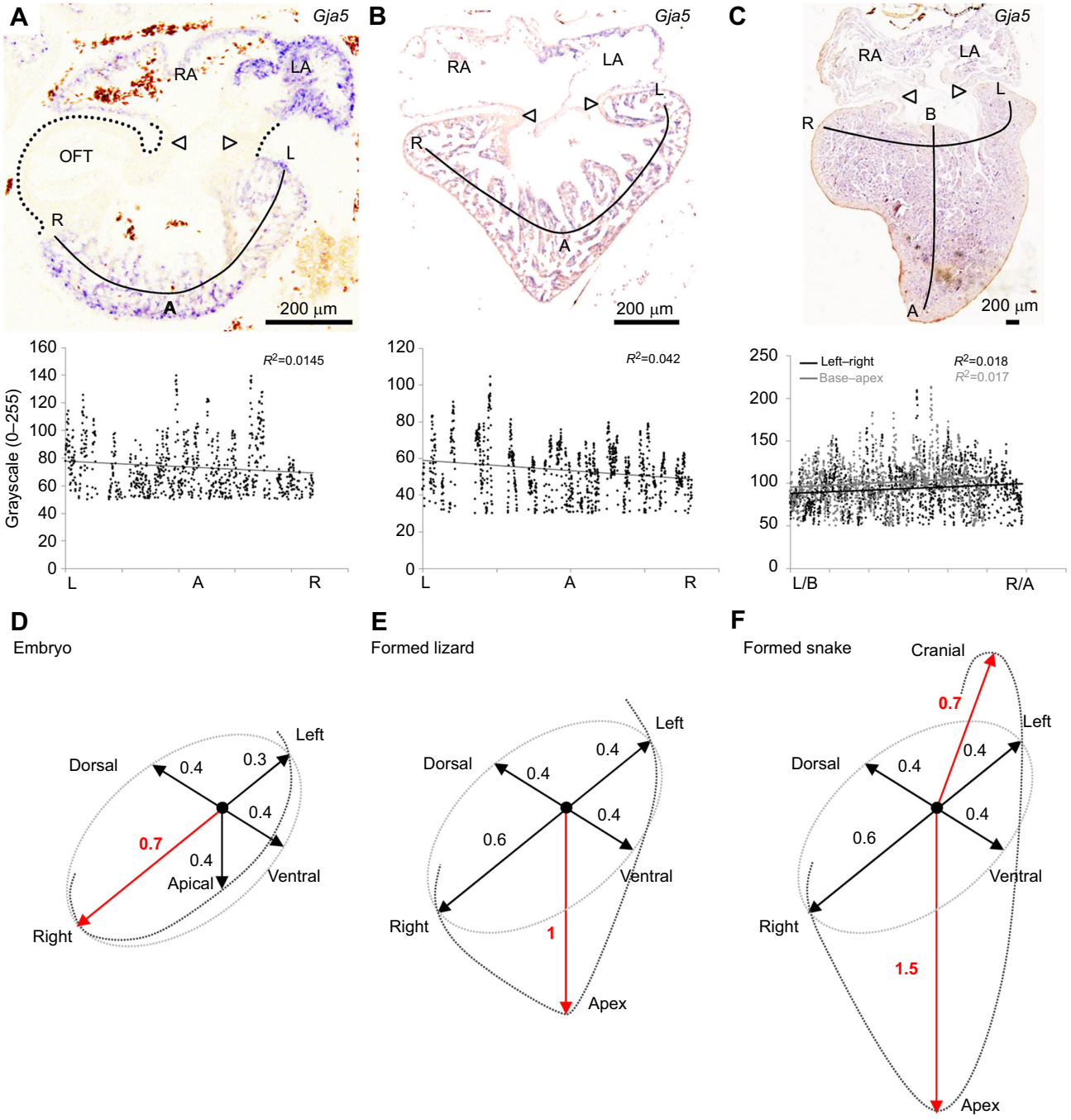

Fig. 1. Expression of *Gja5* during ontogeny of the anole lizard. (A) *Anolis sagrei* at Sanger stage 7 (Sanger et al., 2008). Soon after the ventricle starts to form, it is broad and there is no obvious difference in the expression of *Gja5* from left (L) over the apex (A) to the right (R). *Gja5* was not detected in the atrioventricular canal (open arrowheads) and the myocardial outflow tract (OFT). The graph shows signal intensity along the full line of the photo. (B) *Anolis sagrei* at Sanger stage 17 (Sanger et al., 2008). Close to hatching, the ventricle has elongated and developed a pointy apex (A) and there is no obvious difference in the expression of *Gja5* from left (L) over the apex (A) to the right (R). (C) In the adult *Anolis sagrei*, *Gja5* is not expressed in a gradient along the base (B)–apex(A) axis or the left–right axis. (D–F) The analyses of *Gja5* expression suggest that current spread is isodromotropic across the ventricle; if so, the peripheral-most parts will activate last and the overall activation will seem to propagate along the longest axis of the ventricle. In the broad ventricle of embryonic squamates (D), the extreme right is the furthest from the center of the atrioventricular canal (nodal point of all arrows), and overall activation may proceed from left to right. The values are dimensionless proportions relative to the ventricular left–right width of 1, approximated from the gestational changes and adult anatomy reported previously (Jensen et al., 2013, 2014). Late in gestation and in the formed hearts of lizards (E), the apex is the furthest from the atrioventricular canal, and overall activation may be from the base to the apex. Snakes (F) develop an elongate ventricle with an extensive cranial shoulder on the ventricular left (Jensen et al., 2013), and current may then spread in almost opposite directions towards the apex and the cranial shoulder.

Purkinje system, in mammals and birds (Christoffels et al., 2010; Miquerol et al., 2011). We used one section per heart, cut in the horizontal plane, which included both the atrioventricular canal and the ventricular apex (stage 7, 9, 17, adult), or in the transverse plane of the ventricular base (stage 19). Images of stained hearts were imported into ImageJ version 1.51a, where we first used Enhance Contrast (saturated pixels: 0.4%) and then converted the images to 8-bit and inverted them. Using the Segmented Line tool, we drew a line with 5–10 points, from the ventricular left, over the apical region, to the ventricular right. The grayscale values under the line were retrieved by Plot Profile and then exported. Values below 50 were considered lumen or unstained tissue and were removed. Pearson's correlation was used to correlate staining intensity with anatomical position (in IBM SPSS Statistics version 24). A *P*-value below 0.05 was considered statistically significant. The correlations, irrespective of significance, were considered of limited biological interest if the regression coefficient (R^2) was below 0.1.

Optical mapping and pseudo-electrocardiogram (ECG)

Embryonated eggs of the central bearded dragon and the corn snake were incubated at 28°C and 75% humidity without rotation. At regular intervals, the embryos were carefully removed from the eggs, photographed under a dissecting microscope for staging, and rapidly decapitated. The hearts were then extracted from the embryos with the posterior thoracic wall attached and stained at room temperature for 15 min in di-4-ANEPPS (2.5 mmol l^{-1}, Invitrogen, Carlsbad, CA, USA). After brief rinsing, the samples were pinned at various orientations (anterior, posterior, left and right lateral view) on a silicone-covered bottom of a custom-made dish filled with oxygenated reptilian buffer (see Jensen et al., 2012; pH 7.5) with the addition of 40–60 µmol l^{-1} cytochalasin D (Sedmera et al., 2003) to reduce motion artefacts. Mapping was performed at 0.25–1 kHz using an ULTIMA L setup (SciMedia, Tokyo, Japan) (Sankova et al., 2010). Heart rate, atrioventricular delay and epicardial activation maps were generated with the help of BV_Ana software bundled with the camera as described previously (Sankova et al., 2010).

RESULTS AND DISCUSSION

Gja5 is expressed throughout the ventricle in developing and adult anole lizards

In the stage 7 embryo, the ventricle was broader (left–right) than it was long (caudal–cranial) and the distance from the atrioventricular canal to the extreme right was longer than the distance to the apical region. The same morphology is seen in other squamates at similar stages of development (Jensen et al., 2013). In mammals and birds, *Gja5*, which encodes the low-resistance gap junction protein Cx40, is expressed in the atrioventricular bundle, its bundle branches and the Purkinje network of the specialized conduction system (Dobrzynski et al., 2013). In the stage 7 embryonic anole, *Gja5* was expressed in the atria and ventricle, but not in the atrioventricular canal and the myocardial outflow tract (Fig. 1A). The level of expression was negatively related to the left–right axis ($P<0.001$, $N=821$ pixels), but the squared regression coefficient was miniscule ($R^2=0.02$), showing that almost none of the variation in expression was explained by the left–right axis (Fig. 1A). The stage 9 embryo was analyzed as in Fig. 1A ($P<0.001$, $N=572$ pixels; data not shown), and the squared regression coefficient was also negligible ($R^2=0.02$). By stage 17, close to hatching, the ventricle had elongated and developed a pointed apex (Fig. 1B). From the atrioventricular canal, the distance was now greater to the apex than to the ventricular left and right. There was expression of *Gja5* in the atria and ventricle, but not in the atrioventricular canal and the myocardial outflow tract (Fig. 1B). The level of expression had a significant positive relationship to the left–right axis ($P<0.001$, $N=1078$ pixels), but almost none of the variation in *Gja5* staining intensity was explained by the left–right axis ($R^2=0.04$) (Fig. 1B). The stage 19 specimen was analyzed in the transverse plane ($P<0.016$, $N=683$ pixels; data not shown) and the level of *Gja5* expression did not change from the ventricular left to the right ($R^2=0.01$). In the adult, the shape of the ventricle and the position of the atrioventricular junction was much like that in stage 17 (Fig. 1C). The level of expression of *Gja5* did not change from the ventricular left to the right ($P=0.17$, $N=1769$ pixels), but was positively related to the base to apex axis ($P<0.001$, $N=1509$ pixels), although the squared regression coefficient was again miniscule ($R^2=0.02$) (Fig. 1C). In summary, we did not detect pathways of preferential conduction equivalent to the His bundle or bundle branches of mammals and birds, and propagation of the action potential may spread at similar velocity throughout the ventricular mass. The position of the atrioventricular canal in relation to the ventricular mass, then, may dictate the pattern of ventricular activation (Fig. 1D–F). Next, we tested this hypothesis with optical mapping.

Optical mapping of ventricular activation patterns

The *P. vitticeps* specimens ranged from Sanger stage 6 to 19 (pre-hatching), which corresponded to an increment in crown–rump length from 18.2 to 41.1 mm. Size, developmental stage and gestational duration were not related to heart rate, atrioventricular delay or ventricular activation time (Table 1). This suggests that the mechanistic underpinnings of the measured electrophysiological parameters, like the density of sodium channels and gap junctional proteins, increased in proportion to growth. Similarly, in chickens, heart rate changes very little in the last two-thirds of development and most intervals of the ECG have adult-like values by 5 days of development (Bogue, 1932, 1933).

Table 1. Baseline *ex ovo* cardiac parameters of the specimens used for optical mapping

			f_H		PQ		QRS	
	N	Stage	beats min^{-1}	*P*	ms	*P*	ms	*P*
Pogona vitticeps								
dpo (14–62)	17	6–19	61.7±11.8	0.42	154.4±60.1	0.23	20.3±6.1	0.21
Stage (6–19)	17		61.7±11.8	0.44	154.4±60.1	0.19	20.3±6.1	0.20
CRL (18.2–41.1 mm)	14	6–19	62.7±10.6	0.30	159.9±62.0	0.37	20.6±6.1	0.13
Pantherophis guttatus								
dpo (9–32)	4		76.3±9.5	0.18	130.3±31.2	0.36	14.5±3.4	0.01(+)

Stages according to Sanger et al. (2008). *P*-values are from Pearson correlation. (+), positive relationship; CRL, crown–rump length (mm); dpo, days post-oviposition; f_H, heart rate; PQ, atrioventricular delay; QRS, ventricular activation time.

Journal of Experimental Biology (2018) 221, jeb178400. doi:10.1242/jeb.178400

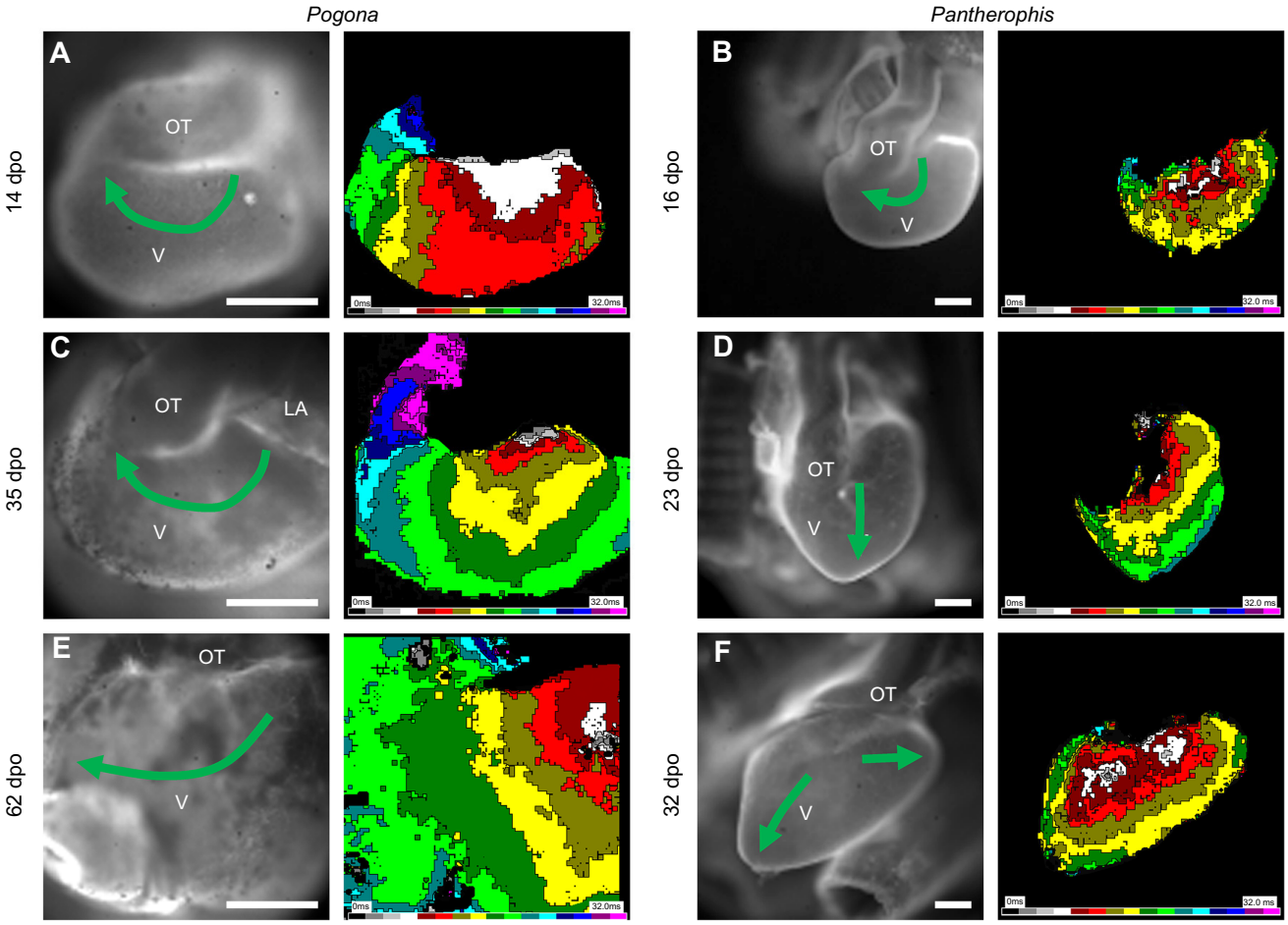

Fig. 2. Developmental changes in ventricular activation patterns in *Pogona vitticeps* (left) and *Pantherophis guttatus* (right). In the early stages with broad ventricles (A,B), the activation wave swept from left to right; this pattern is also present in the older *P. vitticeps* hearts (C,E). In *P. guttatus*, the activation pattern changed to base-to-apex in the more elongate ventricles (D), and in the oldest specimen, two breakthrough sites are visible at the ventricular base (F). A and B are comparable to Fig. 1D; C and E are comparable to Fig. 1E; F is comparable to Fig. 1F. Scale bars: 500 μm. All the maps are rendered at a temporal resolution of 2 ms/color band. dpo, days post-oviposition; OT, outflow tract; V, ventricle.

The hearts of the earliest stages of *P. vitticeps* and *P. guttatus* were broader than they were long and resembled the *A. sagrei* stage 7 embryonic heart. In both *P. vitticeps* and *P. guttatus*, ventricular activation on the ventral and dorsal surface initiated on the left at the ventricular base, where the atrioventricular canal connects to the ventricle (Fig. 2; 14 and 16 days post-oviposition, dpo). From there, the action potentials were propagated in a sweep towards the ventricular right, which was the part of the ventricle that was farthest from the atrioventricular canal. Later stages of *P. guttatus* developed a more elongate ventricle with a pointed caudal apex. The apex was farther from the atrioventricular canal than any other part of the ventricle and the ventral activation pattern was base-to-apex rather than the left-to-right sweep of the younger and broader ventricles (Fig. 2; 23 dpo). In *P.vitticeps*, a base-to-apex pattern of activation also developed in later stages on the ventral surface (Fig. 2; 35 and 62 dpo). On the dorsal surface, there were one or two initial breakthroughs, rather than a single one like on the ventral surface. These breakthroughs were a bit more caudal than on the ventral surface, but still within the region of the ventricular base and far from the apex. Overall, the dorsal pattern of activation was also base-to-apex and resembled the base-to-apex activation patterns reported for the dorsal surface of the adult *A. sagrei* ventricle (Jensen et al., 2012). The heart in the most developed stage of *P. guttatus* was very elongate and had a shoulder on the ventricular left, giving it a second apex on the cranial left. Such a cranial left shoulder was previously shown to develop in the corn snake (Jensen et al., 2013) and is a common feature of the formed hearts of snakes and lizards (Jensen et al., 2014). Activation still originated in the vicinity of the atrioventricular canal and spread simultaneously towards the caudal and cranial apex (Fig. 2; 32 dpo).

Conclusions

In all investigated hearts, the activation initiated in the ventricular base in the vicinity of the atrioventricular canal. The last activated part changed during development from the extreme right initially to the extreme caudal at late stages. This change in activation pattern coincided with a change by growth in shape from initially left–right broad to caudocranial elongate. If the shape of the ventricle largely dictates the pattern of activation, the speed of propagation would be expected to be similar across the trabecular ventricular myocardium. Cx40 allows for fast propagation, and we found that *Gja5*, which encodes Cx40, was essentially homogeneously expressed in the *A. sagrei* ventricle. We propose the ventricular activation pattern in lizards and snakes is largely determined by the shape of the ventricular mass and where the atrioventricular canal connects to the ventricular mass. Such a manner of activation

was probably the basal condition for vertebrates. In contrast, in mammals and birds, the atrioventricular node connects directly to the insulated His–Purkinje network, which ramifies into the apical region predominantly and this part is therefore activated early (Davies and Francis, 1946; Moorman et al., 1998; Sedmera, 2011).

Acknowledgements
We would like to thank Martin Kotal for providing fertilized reptilian eggs.

Competing interests
The authors declare no competing or financial interests.

Author contributions
Conceptualization: M.G., D.S., B.J.; Methodology: M.G., D.S., B.J.; Software: D.S.; Validation: D.S., B.J.; Formal analysis: M.G., D.S., B.J.; Investigation: M.G., D.S., B.J.; Resources: M.G., D.S., B.J.; Writing - original draft: M.G., D.S., B.J.; Writing - review & editing: M.G., D.S., B.J.; Visualization: M.G., B.J.; Supervision: D.S., B.J.

Funding
This work was supported by Ministry of Education, Youth and Sports of the Czech Republic PROGRESS-Q38; Univerzita Karlova v Praze UNCE 204013; Czech Academy of Sciences RVO: 67985823; Grant Agency of the Czech Republic 16-02972S.

References

Boback, S. M., Dichter, E. K. and Mistry, H. L. (2012). A developmental staging series for the African house snake, *Boaedon (Lamprophis) fuliginosus*. *Zoology* **115**, 38-46.
Bogue, J. Y. (1932). The heart rate of the developing chick. *J. Exp. Biol.* **9**, 351-358.
Bogue, J. Y. (1933). The electrocardiogram of the developing chick. *J. Exp. Biol.* **10**, 286-292.
Burggren, W., Farrell, A. P., Lillywhite, H. B. (1998). Vertebrate cardiovascular systems. Compr. Physiol. 2011, Supplement 30, *Handbook of Physiology*, *Comparative Physiology*, pp. 215-308. Chichester: John Wiley & Sons, Inc.
Christoffels, V. M., Smits, G. J., Kispert, A. and Moorman, A. F. M. (2010). Development of the pacemaker tissues of the heart. *Circ. Res.* **106**, 240-254.
Davies, F. and Francis, E. T. B. (1946). The conducting system of the vertebrate heart. *Biol. Rev.* **21**, 173-188.
Dobrzynski, H., Anderson, R. H., Atkinson, A., Borbas, Z., D'Souza, A., Fraser, J. F., Inada, S., Logantha, S. J. R. J., Monfredi, O., Morris, G. M. et al. (2013). Structure, function and clinical relevance of the cardiac conduction system, including the atrioventricular ring and outflow tract tissues. *Pharmacol. Ther.* **139**, 260-288.
Jensen, B., Boukens, B. J. D., Postma, A. V., Gunst, Q. D., van den Hoff, M. J. B., Moorman, A. F. M., Wang, T. and Christoffels, V. M. (2012). Identifying the evolutionary building blocks of the cardiac conduction system. *PLoS ONE* **7**, e44231.
Jensen, B., van den Berg, G., van den Doel, R., Oostra, R.-J., Wang, T. and Moorman, A. F. M. (2013). Development of the hearts of lizards and snakes and perspectives to cardiac evolution. *PLoS ONE* **8**, e63651.
Jensen, B., Moorman, A. F. M. and Wang, T. (2014). Structure and function of the hearts of lizards and snakes. *Biol. Rev.* **89**, 302-336.
Jensen, B., Vesterskov, S., Boukens, B. J., Nielsen, J. M., Moorman, A. F. M., Christoffels, V. M. and Wang, T. (2017). Morpho-functional characterization of the systemic venous pole of the reptile heart. *Sci. Rep.* **7**, 6644.
Jensen, B., Boukens, B. J., Crossley, D. A., Conner, J., Mohan, R. A., van Duijvenboden, K., Postma, A. V., Gloschat, C. R., Elsey, R. M., Sedmera, D. et al. (2018). Specialized impulse conduction pathway in the alligator heart. *eLife* **7**, e32120.
Miquerol, L., Beyer, S. and Kelly, R. G. (2011). Establishment of the mouse ventricular conduction system. *Cardiovasc. Res.* **91**, 232-242.
Moorman, A. F. M., de Jong, F., Denyn, M. M. F. J. and Lamers, W. H. (1998). Development of the cardiac conduction system. *Circ. Res.* **82**, 629-644.
Park, D. S. and Fishman, G. I. (2017). Development and function of the cardiac conduction system in health and disease. *J. Cardiovasc. Dev. Dis.* **4**.
Sanger, T. J., Losos, J. B. and Gibson-Brown, J. J. (2008). A developmental staging series for the lizard genus *Anolis*: a new system for the integration of evolution, development, and ecology. *J. Morphol.* **269**, 129-137.
Sankova, B., Machalek, J. and Sedmera, D. (2010). Effects of mechanical loading on early conduction system differentiation in the chick. *Am. J. Physiol. Heart Circ. Physiol.* **298**, H1571-H1576.
Sedmera, D. (2011). Function and form in the developing cardiovascular system. *Cardiovasc. Res.* **91**, 252-259.
Sedmera, D., Reckova, M., DeAlmeida, A., Sedmerova, M., Biermann, M., Volejnik, J., Sarre, A., Raddatz, E., McCarthy, R. A., Gourdie, R. G. et al. (2003). Functional and morphological evidence for a ventricular conduction system in zebrafish and *Xenopus* hearts. *Am. J. Physiol. Heart Circ. Physiol.* **284**, H1152-H1160.